Shahrood University of Technology

Journal of Hydraulic and Water Engineering (JHWE)

Journal homepage: https://jhwe.shahroodut.ac.ir/

Iranian Hydraulic Association (IHA)

Investigating Effect of Changing Vegetation Height with Irregular Layout on Reduction of Waves using Flow-3D Numerical Model

S. A. Ghaheri Nejad [1*] , M. Behdarvandi Askar [2]

[1*] Graduated from Offshore Structures, Department of Offshore Structures, Faculty of Marine Engineering, Khorramshahr University of Marine Science and Technology, Iran.
[2] Associate Professor in Department of Marine Structures, Khorramshahr University of Marine Science and Technology, Iran.

Article Info

Article history:

Received: 14 March 2023
Received in revised form: 16 April 2023
Accepted: 5 June 2023
Published online: 8 June 2023

DOI:
10.22044/JHWE.2023.12844.1004

Keywords
Green belt
Geometric layout
Vegetation
Irregular layout
Regular layout

Abstract

Coastal plants can have a significant effect on the damping of the waves on the shores of rivers and seas. Its effectiveness depends on various factors including their height, layouts, geometry, etc. In this study, the effect of changing vegetation heights with irregular arrangement on wave reduction is investigated using the numerical model Flow 3D. For this purpose, a model of a channel with a specific dimension is simulated, and the three-layout vegetation, namely long-short, short-to-long, and zigzag layouts under four different waves, all of which are linear waveforms. The measurements of the wave height at four different points along the canal indicate that the behavior of waves in dealing with different layers follows a steady pattern, and the change in vegetation geometry can greatly lead to increase in damping waves. From this research work, it can be concluded that in order to achieve maximum damping in vegetation with variable height, it is necessary that the maximum level of lateral obstruction is at the beginning of the cover, and in the face of maximum wave energy.

1. Introduction

One of the factors that can have a significant effect on the performance of coastal plants is how they are located and their geometry. The geometric arrangement of these plants with variable height and how they change their height along the shoreline or perpendicular to the shoreline can greatly affect the damping of the waves (Asano, 1988; Asano et al., 1992; Dubi, 1995; Tavakoli et al., 2022). In addition to absorbing wave energy reaching the shore, these plants play an important role in protecting beaches from erosion. The study of the effect of change in height, diameter, and stalk distances greatly helps to predict and estimate wave behavior when entering the shore (Shih et al., 2022; Zhang et al., 2022). In addition, experience has shown that different altitude states can cause changes in wave damping, which is the goal of the present study. According to studies conducted in the recent decades on vegetation and its effects on wave damping, many variables can always be

* *Corresponding author. E-mail address: sazehenteghal@yahoo.com, Tel:+ 989166169813.*

considered involved in depreciation that have been studied by various researchers (Best et al., 2022; Hu et al., 2022; Ma et al., 2023). Meanwhile, the geometric arrangement of the stems with variable heights can also be considered as one of the important factors that knowing its effects can be a great help in studying plant cover. Therefore, in this research work, an attempt has been made to conduct a complete study on this issue, relying on the achievements of the researchers. The results of the researchers in this field indicate that, in general, vegetation increases current resistance, controls flow, and affects the rate of erosion and sedimentation (Fathi-Moghadam et al., 2011). Also the use of vegetation according to the goals of each project depends on environmental conditions, soil degradability, plant type, planting method, and biological stabilization and vegetation maintenance management (Dean, 1979; Dean and Dalrymple, 1991). The first research work that was conducted to establish a relationship between the hydraulic roughness of the flow with depth and speed, as well as the type and height of vegetation, began in the laboratory of the Soil Protection Organization of the state of South Carolina in Spartarg, USA.

Li and Shen (1973) examined the effect of plant resistance with different cylindrical stems in the immersive state. The results showed that different patterns of placement of cylindrical stems had a significant impact on Dubai. In addition, physical models were used to determine the coefficient of roughness with stiff cylindrical stems, so that part of this research work, for the calculation of the various plants in the plant growth area, was planned. Li and Shen (1973) carried out an experimental study for calculating the coefficient of friction for a single plant in a category with CWR, and also the calculation of the coefficient of roughness for vegetation (f_P). Study of Mukherjee et al. (2023) indicated that forest density is more effective than tree rigidity at reducing the onshore energy flux of tsunamis. Approximately 50 to 200 percent increase in wave damping per meter is observed in non-immersive cover conditions with stem length ratio (LS) to wave height (H) more than one, compared to immersive cover conditions (LS / H = 0.75) (Asano et al., 1992; Cooper, 2005). Experimental laboratory studies have shown that wave energy loss depends on the density of the forest cover (including the layout and width of the cover) and the diameter of the tree trunk (van Wesenbeeck et al., 2022).

A combined, quasi-three-dimensional and laboratory numerical study was conducted to analyze, compile, and determine the drag formula derived from vegetation. The coating is simulated in two immersive and non-immersive modes with two types of flexible stem and hard stem without flexibility. In this study, the "Cantilever Base" theory was used to calculate the amount of deviation and drag caused by flexible vegetation (Erduran and Kutija, 2003). Numerical and laboratory studies on the damping energy of wave energy hit by mangrove coastal forests revealed the effectiveness of this method in coastal protection (Imamura et al., 2006).

2.Materials and Methods

2.1. Flow-3D model

In this study, we used the Flow-3D model to study the effect of changing vegetation height with irregular layout on the reduction of waves. This model is a powerful computational fluid dynamics (CFD) software package that is used to simulate fluid flows and related phenomena in a variety of industries such as hydraulic, marine, and manufacturing. The software is based on the finite volume method, and is capable of simulating complex fluid dynamics problems involving free surfaces, multi-phase flows, and fluid-structure interactions.

The Flow-3D model is made up of three main components: the geometry model, the physics model, and the numerical model. The geometry model defines the physical domain of the problem and is typically created using a CAD software package. The physics model describes the fluid dynamics and other physical

phenomena that are being simulated, such as heat transfer, chemical reactions, and turbulence. The numerical model uses numerical methods to solve the governing equations of fluid dynamics and other physical phenomena.

Flow-3D offers a wide range of advanced features including particle tracking, surface tension modeling, and fluid-structure interaction modeling. It also includes a user-friendly interface that allows users to easily set up and run simulations, as well as to visualize and analyze the results.

Overall, the Flow-3D model is a highly sophisticated tool that is used by the engineers and researchers to study complex fluid dynamics problems, and to design and optimize real-world systems and processes.

2.2. Design and specifications of geometry of the model used

The study used a 488,0 cm long and 108 cm wide phloem previously used by Dr. Daniel T. Cox and Wee Cheng Woo at the University of Oregon in the United States to study the effect of plant density on variable altitude damping. In the present study, first, the flow was modeled using the Flow-3D model, and after calibration and validation, the same geometry has been used to study the geometric arrangement of vegetation with altitude variable on wave damping.

Figure 1 shows a view of this geometry, based on the research work by Dr. Daniel T. Cox and Wee Cheng Woo, redesigned by Auto CAD, to validate the model in Flow-3D software.

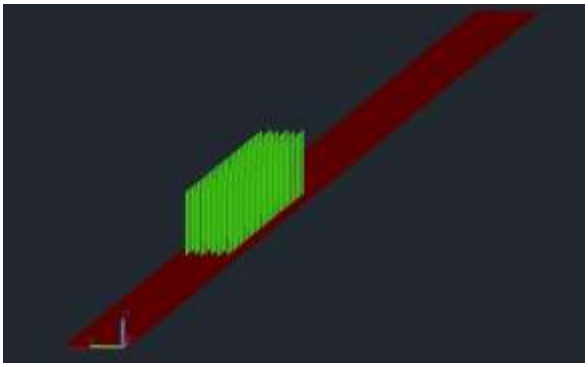

Figure 1. Geometry used by Wu and Cox (2016) to study the effect of plant density with variable height on wave damping.

2.3. Waves and vegetation under study

For this study, 4 different types of air type, with period, index height and other different specifications are considered. The length and diameter of the stems used in this study are in accordance with Table 1. In addition, the specifications of these waves are listed in Table 2.

Table 1. Diameter and height of the stems.

Height of stems (mm)	6	8	10	12	14
Diameter (mm)	5	5	5	5	5

Table 2. Specifications of the studied waves

No.	H (cm)	T (s)	Hs (cm)	kh	αk	Re	Kc	Ur
1	12	0.4	1.49	1.04	0.19	590	10	1
2	12	0.6	1.87	0.49	0.12	540	13	3
3	12	1	2.82	0.76	0.09	690	28	16
4	12	1.4	3.42	0.52	0.07	810	45	42

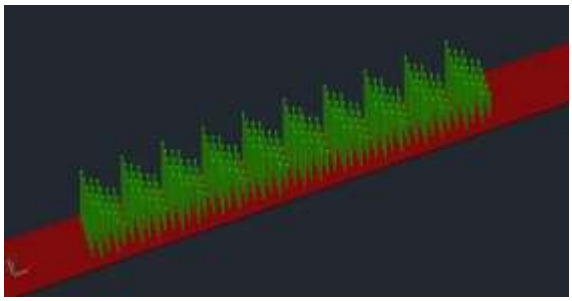

Figure 2. 3D view related to descending mode.

Figure 2. Two-dimensional view of long mode.

2.4. Research scenarios

The layout of this study is rigid cylindrical stems with regular spatial arrangement that are studied in three modes: long to short, short to long, and zigzag. The two-dimensional and

three-dimensional view of these layouts is shown in the following sections.

(a) **Short to long mode**

In this case, the stems in the first row have the shortest height equal to 6 cm, and the second to fifth rows have the height of 8 cm, 10 cm, 12 cm, and 14 cm, respectively. This geometric pattern continues alternately from the starting point of the cover, i.e. at a distance of 1.3 m^3 from the beginning of the channel, to 90 cm afterwards. Figures 5 and 6 show the side and three-dimensional views of this arrangement, respectively.

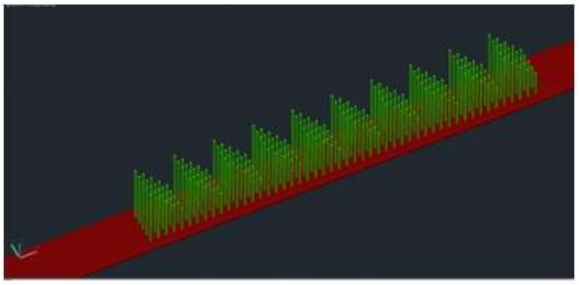

Figure 4. Three-dimensional view long to short mode.

Figure 5. Two-dimensional view short to long mode.

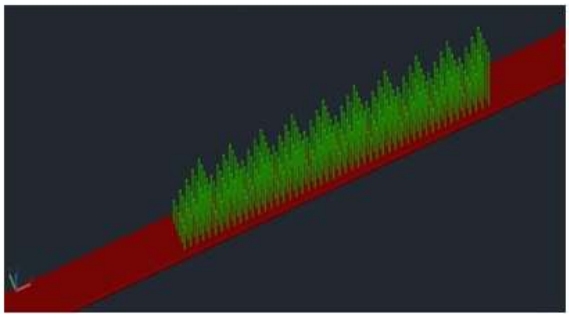

Figure 6. Three-dimensional view of long to short mode.

(b) Zigzag mode

In this case, the length of the stems in the first row varies from left to right, and from large to small. In the same way, the stems of the second row, in contrast to the first row, change from right to left, and from large to small. This geometric pattern continues alternately from the starting point of the cover, i.e., at a distance of 1.3 m from the beginning of the channel, to 90 cm afterwards. Figures 7 and 8 show the side and three-dimensional views of this arrangement, respectively.

Table 3. Number and dimensions of mesh considered and average error rate.

No.	Main network dimentions (m)	Subsidary network dimentions (m)	Total number of network cells (m)	Avarge eroor (%)
1	0.01	0.003	904, 186	15.4
2	0.008	0.002	2785, 320	5.1
3	0.005	0.002	3579, 720	2.5

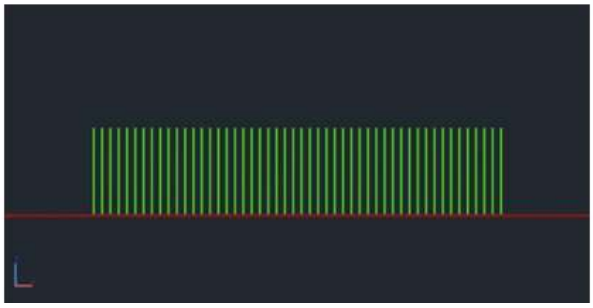

Figure 7. Two-dimensional view.

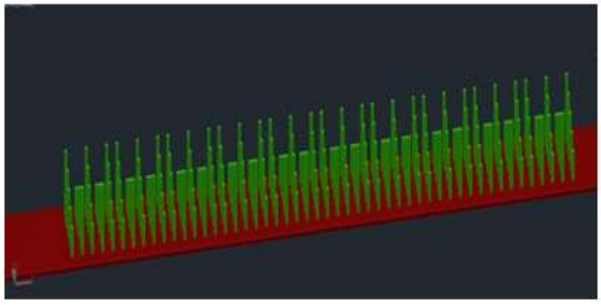

Figure 8. Three-dimensional zigzag view.

3. Results and Discussion

3.1. Calibration and validation of numerical model

For calibration and validation, based on the studies of Wu and Cox (2016), a cover consisting of 150 stems with a height of 14 cm and a diameter of 5 mm with a length of 90 cm from a flow with a length of 4.8 m8 and a width of 10.4 cm is created. The wave irradiated to

the cover is of linear type with a height of 1.87 cm with a period of 0.6 s. After designing the model using AutoCAD software and transferring the model to the Flow-3D, it is necessary to select the appropriate mesh network so that the solution network, in addition to having sufficient accuracy, is also time-consuming and economical. Due to the long length of the model and its low width, as well as the small diameter of the stems, it is necessary to create two mesh networks, so that while maintaining accuracy, the network resolution time is minimized. Table 3 shows the number and dimensions of the meshes considered and the average error rate of each. It should be noted that two mesh networks have been used for this research work, the first network from the beginning to the end of the channel, and the second network only includes the beginning to the end of vegetation.

As it can be seen in Table 3, the accuracy can be increased by minimizing the dimensions of the computational network but it should also be noted that shrinking the dimensions of the grid can lead to an increase in the number of computational cells, and therefore, increases the time required to solve this network.

In Table 3, number 3 mode is the most appropriate meshing mode, because in addition to good accuracy, the time required to solve it is also acceptable. It should be noted that by taking these dimensions into account, the calculation error can be reduced to less than this value but because it is time consuming, it is not economical to do so.

After designing the channel and simulating the required conditions, as well as finding the appropriate dimensions for the computational network, we analyzed the output results, and compared them with the results of his research by Cheng Wu and Daniel T. Cox. According to the four waves selected for testing, the second mode wave presented in Table 1 was used for calibration and validation. In this study, the wave height ratio at each point relative to the index wave height was referred to as the transfer parameter (K_v):

$$K_v = \frac{H(x)}{H_s} \quad (1)$$

Figure 9 shows how the transfer parameter (Kv) changes at the four measured points, and in this measurement, the friction of the floor and walls is ignored. This figure, which is the most important conclusion in the present study, actually shows how the waves die after entering the vegetation range and the severity of the depreciation caused by the vegetation without considering floor and wall polishing. Figure 9 shows the height of the waves at four points, X = 0, X = 0.2, X = 0.5, X = 0.9 had been measured. Error values were calculated after extracting these values from Cheng Wu and Daniel T. Cox's research, as well as CFD height calculation. These values are given in Table 4.

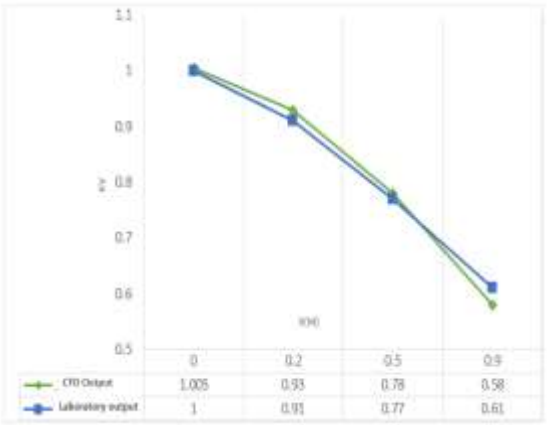

Figure 9. Comparison of the results of the studies of Wu and Cox (2016) (Laboratory), with the results of the present study (CFD).

Table 4. Results of the studies of Wu and Cox (2016) with the results of the present study.

No.	CFD Output		Laboratory Output	
	X (m)	Kv	X (m)	Kv
1	0	1.005	0	1
2	0.2	0.94	0.2	0.91
3	0.5	0.78	0.5	0.77
4	0.9	0.58	0.9	0.61

Table 5. Calculation of error rate in the present study compared to the study of Wu and Cox (2016).

No.	Kv		Error (%)
	X (m)	CFD Output	Laboratory Output

1	0	1.005	1	0.5
2	0.2	0.94	0.91	3.29
3	0.5	0.78	0.77	1.29
4	0.9	0.58	0.61	4.91

As it can be seen in Table 5, the difference between the values measured in the laboratory by Wu and Daniel T. Cox, and the values calculated by the CFD method, shows a small difference of less than 5%. Based on this issue and ensuring the accuracy of the model used, it is possible to use this model to study the effect of geometric arrangement of vegetation with variable height on wave damping.

3.2. Analysis of numerical model results

According to Table 1, four different waves are considered in this study, and for each wavelength, these three modes of arrangement are examined.

3.2.1. Wave mode No. 1

Figure 10 shows the effect of the three modes of high-altitude to short, short to long, and zigzag elevation on the damping of wave number 1. In this case, it is observed that the highest damping is related to the long to short mode, and then the zigzag mode has the highest damping; and it is also observed that the short to long mode causes the lowest damping. Also in the first measurement period, it is observed that the wave increases slightly in height, which is due to the principle of continuity; this state is observed in all layouts.

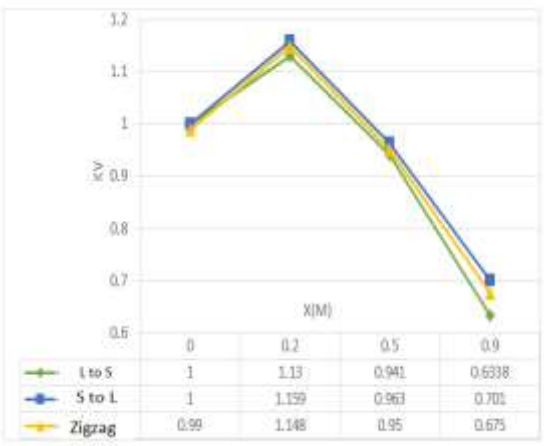

Figure10. Effect of vegetation under the effect of wave number 1.

According to Figure 10, the minimum value of the Kv parameter that the wave reaches when passing through the cover is equal to 0.634, which is related to the arrangement of long to short height at the end of the cover; and the maximum value of the Kv parameter. For short to long altitude arrangement, which is measured at the second point and is equal to 1.159, the height of the wave at each point of measurement is obtained by multiplying the Kv parameter at the initial wave height.
To better understand damping for each sub-mode, the damping percentage parameter is defined according to Equation (2):

$$POD = (1 - K_V) * 100 \qquad (2)$$

In relation (1), the POD is the damping percentage and Kv is equal to the value of this parameter at the last measuring point. The results of the damping percentage related to the elevation arrangement due to wave number 1 are listed in Table 6.

Table 6. Extinction percentage of vegetation related to the effect of wave number 1.

Arrangement	POD%
L TO S	36.62
S TO L	29.9
Zigzag	32.50

As shown in Table 6, the highest damping percentage is for short to high altitude layout,

and the lowest percentage is for short to long altitude layout.

3.2.2. Wave mode No. 2

In this case, by selecting wave number 2 as the base wave, these three height arrangements are examined in order. This wave, which is of the Erie type, height and period, and other features are listed in Table 1. Figure 11 shows the effect of three high-altitude to short, short to long, and zigzag altitudes on wave damping.

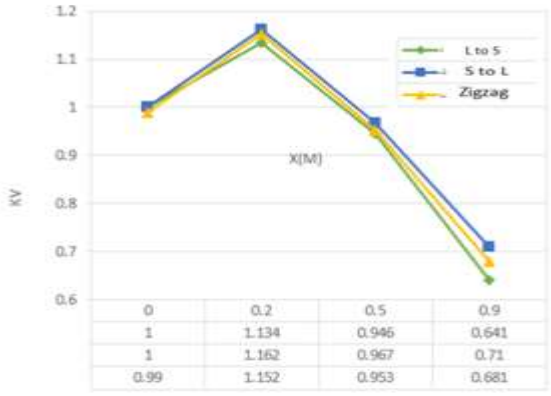

Figure 11. Effect of three high-altitude to short, short to long, and zigzag altitudes on wave damping.

As shown in the figure, the long-to-short layout results in the highest damping of the three available modes, and the lowest damping occurs by short-to-long layout. In this case, the minimum value of the Kv parameter that the wave reaches when passing through the cover is equal to 0.641, which is related to the arrangement of long sub-height to short and at the end of the cover; and the maximum value of Kv parameter, it is a short to long altitude arrangement, which is the second measurement point and is equal to 1.162. The results for the damping percentage of the regular state sub-states with the same intervals are given in Table 7.

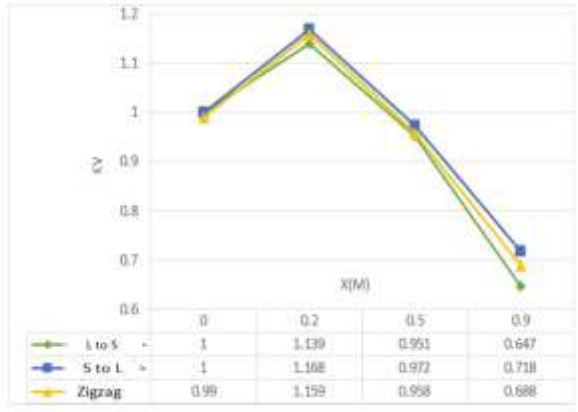

Figure 12. Effect of vegetation under the effect of wave number 3 on the kv parameter.

In Table 7, it is observed that the same damping pattern under wave number 1 is repeated in this case, and the highest and lowest damping are performed under long to short and short to long arrangements, respectively.

Table 7. Extinction percentage of vegetation related to the effect of wave number 2.

Arrangement	POD%
L TO S	35.9
S TO L	29
Zigzag	31.9

3.2.3. Wave mode 3

In this case, by selecting wave number 3 as the base wave, these three altitude arrangements are examined in order. This wave, which is of the Erie type, height and period and other features are listed in Table 1. The simulation and its results are in the form of Figure 12.

As shown in Figure 12, under this wavelength, the minimum value of the Kv parameter that the wave reaches when passing through the coating is 0.647, which is related to the arrangement of high to short height and at the end of the coating; and the maximum value of the Kv parameter is for short to long altitude arrangement, which is at the second point of measurement and is equal to 0.168. In this case, the highest damping is related to long to short altitude arrangement and the lowest damping is

related to short to long altitude arrangement. The results of the damping percentage of these arrangements are listed in Table 8 below Wave 3:

Table 8. Extinction percentage of vegetation related to the effect of wave number 3.

Arrangement	POD%
L TO S	35.3
S TO L	28.2
Zigzag	32.2

According to Table 8, the highest damping is observed for short to long layout and the lowest for short to long layout.

3.2.4. Wave mode No. 4

In this case, by selecting the wave number 4 as the base wave, these arrangements are examined in order. This wave, which is of the Erie type, height and period and other features are listed in Table 1. The simulation and its results are in the form of Figure 13.

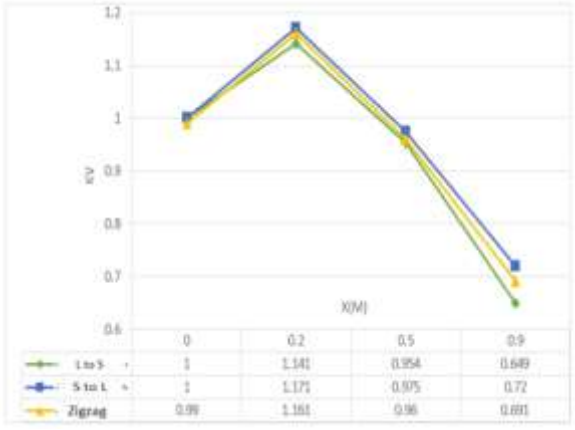

Figure 13. Effect of vegetation under the effect of wave number 4.

According to Figure 12, the minimum value of the Kv parameter that the wave reaches when passing through the cover is equal to 0.649, which is related to the high to short height arrangement at the end of the cover; and the maximum value of the Kv parameter, it is a short to long elevation arrangement, which is measured at the second point and is equal to 1.171. In this case, the highest damping is related to long to short altitude arrangement and the lowest damping is related to short to long altitude arrangement. The results of the damping percentage for these three elevation arrangements are given in Table 9. It shows that the highest and lowest damages are related to long to short and short to long arrangement, respectively.

Table 9. Extinction percentage of vegetation related to the effect of wave number 4.

Arrangement	POD%
L TO S	35.1
S TO L	28
Zigzag	30.9

By selecting four different wave modes and three different altitude layouts, the above simulation is performed. In each arrangement, measurements were made at four common and identical points for the wave height, and finally, by obtaining the Kv coefficient, the damping ratio of the wave due to the presence of the coating along the vegetation was presented in the form of the above figures. Carefully in the figure, it can be seen that a change in the geometric arrangement of the vegetation can lead to a change in the damping of the waves reaching the shore.

In addition to the geometric arrangement of the studied coating, this damping depends on other factors such as stem thickness, flexibility, density, stem height, and cover width, which are out of the scope of this study. As the wave hits the cover, since these stems have a surface against the flow, so according to the law of continuity, the existing surface for the flow to pass decreases, and as a result the wave height and Kv parameter increase slightly, and after the wave loses a significant amount of energy, it is observed that the parameter Kv and consequently the height of the wave decreases, until at the last point of

measurement, which is the same point m = 0.9 m. It reaches its minimum value.

With the start of the process of radiating the wave to the cover, and after the wave hits the first of these stems located in the channel, we see an increase in the height of the wave. This phenomenon is due to the principle of flow continuity and is directly related to the area of the part of the stems that are exposed to wave and current movement. This area, called the lateral inhibition level, is a very important factor in wave damping. Carefully in the figures, it can be seen that the difference between the different geometric arrangements, which are in fact the same as the level of lateral blocking of the coverage at each section, causes a change in the damping and depreciation rate of the waves. From these observations, it can be seen that at the moment the wave hits the cover, the wave energy has its maximum amount; over time, the wave will pass through the cover and lose some of its energy, the effect of the lateral inhibition level will be greater and clearer. From this research work, it can be concluded that in order to achieve maximum damping in vegetation with variable height, it is necessary that the maximum level of lateral obstruction is at the beginning of the cover, and in the face of maximum wave energy. His research by Cheng Wu and Daniel T. Cox (2015) showed that by managing the level of lateral inhibition by changing the density or changing the geometry of the coating, other parameters effective in damping the waves in plant coatings can be fixed. It greatly increased the damping.

Data Availability

The data used to support the findings of this study is available from the corresponding author upon request.

Conflicts of Interest

The authors declare that they have no conflicts of interest regarding the publication of this paper.

References

Asano, T., 1988. Wave damping characteristics due to seaweed, Proc. 35th Conf. on Coastal Engrg., 1988.

Asano, T., Deguchi, H., and Kobayashi, N., 1992. Interaction between water waves and vegetation, Coastal Engineering 1992, pp. 2709-2723.

Best, Ü.S., van der Wegen, M., Dijkstra, J., Reyns, J., van Prooijen, B.C., and Roelvink, D., 2022. Wave attenuation potential, sediment properties and mangrove growth dynamics data over Guyana's intertidal mudflats: assessing the potential of mangrove restoration works. *Earth System Science Data*, 14(5), pp. 2445-2462.

Cooper, N.J., 2005. Wave dissipation across intertidal surfaces in the Wash tidal inlet, eastern England. *Journal of Coastal Research*, 21(1), pp. 28-40.

Dean, R., 1979. Effects of vegetation on shoreline erosional processes. p. 416–426. *R E. Greeson, J, R, Clark, and J*, 1(2).

Dean, R.G., and Dalrymple, R.A., 1991. Water wave mechanics for engineers and scientists, 2. world scientific publishing company.

Dubi, A., 1995. Damping of water waves by submerged vegetation–a case study on Laminaria hyperborea. Dr. Ing, Thesis, Department of Structural Engineering, NTNU/SINTEF-NHL, N-7034 Trondheim, Norway., Institute: Universitetet i Trondheim (Norway) Publisher.

Erduran, K., and Kutija, V., 2003. Quasi-three-dimensional numerical model for flow through flexible, rigid, submerged and non-submerged vegetation. *Journal of Hydroinformatics*, 5(3), pp. 189-202.

Fathi-Moghadam, M., Kashefipour, M., Ebrahimi, N., and Emamgholizadeh, S., 2011. Physical and numerical modeling of submerged vegetation roughness in rivers and flood plains. *Journal of Hydrologic Engineering*, 16(11), pp. 858-864.

Hu, Z., Lian, S., Zitman, T., Wang, H., He, Z., Wei, H., Ren, L., Uijttewaal, W., and Suzuki, T., 2022. Wave breaking induced by opposing currents in submerged vegetation canopies. *Water Resources Research*, 58(4), pp. e2021WR031121.

Imamura, M. et al., 2006. Current status of hematopoietic cell transplantation for adult patients with hematologic diseases and solid tumors in Japan. *International journal of hematology*, 83, pp. 164-178.

Li, R.-M., and Shen, H.W., 1973. Effect of tall vegetations on flow and sediment. *Journal of the hydraulics division*, 99(5), pp. 793-814.

Ma, Y. et al., 2023. Wave attenuation by flattened vegetation (Scirpus mariqueter). *Frontiers in Marine Science*, 10, pp. 571.

Mukherjee, A., Cajas, J.C., Houzeaux, G., Lehmkuhl, O., Suckale, J., and Marras, S., 2023. Forest density is more effective than tree rigidity at reducing the onshore energy flux of tsunamis. *Coastal Engineering*, 182, pp. 104286.

Shih, R.-S., Li, C.-Y., Weng, W.-K., and Lin, C.-H., 2022. Relative Energy Variation Characteristics Considering Interaction between Waves and Vegetation Structure. *Water*, 14(16), pp. 2567.

Tavakoli, S., Shaghaghi, P., Mancini, S., De Luca, F., and Dashtimanesh, A., 2022. Wake waves of a planing boat: An experimental model. *Physics of Fluids*, 34(3), pp. 037104.

van Wesenbeeck, B.K., Wolters, G., Antolínez, J.A., Kalloe, S.A., Hofland, B., de Boer, W.P., Çete, C., and Bouma, T.J., 2022. Wave attenuation through forests under extreme conditions. *Sci Rep*, 12(1), pp. 1884.

Wu, W.-C., and Cox, D.T., 2016. Effects of vertical variation in vegetation density on wave attenuation. *Journal of Waterway, Port, Coastal, and Ocean Engineering*, 142(2), pp. 04015020.

Zhang, X., Lin, P., and Nepf, H., 2022. A wave damping model for flexible marsh plants with leaves considering linear to weakly nonlinear wave conditions. *Coastal Engineering*, 175, pp. 104124.